Mineralogical Magazine, August 2018, Vol. 82(4), pp. 863–876

Fluorarrojadite-(BaNa), $BaNa_4CaFe_{13}Al(PO_4)_{11}(PO_3OH)F_2$, a new member of the arrojadite group from Gemerská Poloma, Slovakia

Martin Števko[1,*], Jiří Sejkora[1], Pavel Uher[2], Fernando Cámara[3], Radek Škoda[4] and Tomáš Vaculovič[5]

[1] Department of Mineralogy and Petrology, National Museum, Cirkusová 1740, 193 00 Prague 9 - Horní Počernice, Czech Republic
[2] Department of Mineralogy and Petrology, Faculty of Natural Sciences, Comenius University, Ilkovičova 6, 842 15 Bratislava, Slovak Republic
[3] Dipartimento di Scienze della Terra "A. Desio", Università di Milano, via Mangiagalli 34, 20133 Milano, Italy
[4] Department of Geological Sciences, Faculty of Science, Masaryk University, Kotlářská 2, 611 37 Brno, Czech Republic
[5] Department of Chemistry, Faculty of Science, Masaryk University, Kotlářská 2, 611 37 Brno, Czech Republic

[*Received 26 April 2017; Accepted 24 July 2017; Associate Editor: G. Diego Gatta*]

ABSTRACT

The new mineral fluorarrojadite-(BaNa), ideally $BaNa_4CaFe_{13}Al(PO_4)_{11}(PO_3OH)F_2$ was found on the dump of Elisabeth adit near Gemerská Poloma, Slovakia. It occurs in hydrothermal quartz veins intersecting highly fractionated, topaz–zinnwaldite S-type leucogranite. Fluorarrojadite-(BaNa) is associated with fluorapatite, 'fluordickinsonite-(BaNa)', triplite, viitaniemiite and minor amounts of other minerals. It forms fine-grained irregular aggregates up to 4 cm x 2 cm, which consist of individual anhedral grains up to 0.01 mm in size. It has a yellowish-brown to greenish-yellow colour, very pale yellow streak and a vitreous to greasy lustre. Mohs hardness is ~4½ to 5. The fracture is irregular and the tenacity is brittle. The measured density is 3.61(2) g cm^{-3} and calculated density is 3.650 g cm^{-3}. Fluorarrojadite-(BaNa) is biaxial (+) and nonpleochroic. The calculated refractive index based on empirical formula is 1.674. The empirical formula (based on 47 O and 3 (OH + F) apfu) is $^{A1}(Ba_{0.65}K_{0.35})_{\Sigma1.00}{}^{A2}Na_{0.35}{}^{B1}(Na_{0.54}Fe_{0.46})_{\Sigma1.00}{}^{B2}Na_{0.54}{}^{Ca}(Ca_{0.74}Sr_{0.20}Pb_{0.02}Ba_{0.04})_{\Sigma1.00}Na_2{}^{Na3}Na_{0.46}{}^{M}(Fe_{7.16}Mn_{5.17}Li_{0.37}Mg_{0.12}Sc_{0.08}Zn_{0.06}Ga_{0.02}Ti_{0.02})_{\Sigma13.00}Al_{1.02}P_{11}O_{44}PO_{3.46}(OH)_{0.54}{}^{W}(F_{1.54}OH_{0.46})$. Fluorarrojadite-(BaNa) is monoclinic, space group *Cc*, $a = 16.563(1)$ Å, $b = 10.0476(6)$ Å, $c = 24.669(1)$ Å, $\beta = 105.452(4)°$, $V = 3957.5(4)$ Å^3 and $Z = 4$. The seven strongest reflections in the powder X-ray diffraction pattern are [d_{obs} in Å, (I), *hkl*]: 3.412, (21), 116; 3.224, (37), 206; 3.040, (100), 42$\bar{4}$; 2.8499, (22), 33$\bar{3}$; 2.7135, (56), 226; 2.5563, (33), 028 and 424; 2.5117, (23), 040. The new mineral is named according to the nomenclature scheme of arrojadite-group minerals, approved by the IMA CNMNC. In fluorarrojadite-(BaNa), Fe^{2+} is a dominant cation at the *M* site (so the root-name is arrojadite) and two suffixes are added to the root-name according to the dominant cation of the dominant valence state at the *A*1 (Ba^{2+}) and *B*1 sites (Na^+). A prefix fluor is added to the root-name as F^- is dominant over $(OH)^-$ at the *W* site.

Keywords: fluorarrojadite-(BaNa), new mineral, arrojadite group, phosphates, Raman spectroscopy, S-type granite, Gemerská Poloma, Slovakia.

Introduction

Fluorarrojadite-(BaNa), ideally $BaNa_4CaFe_{13}Al(PO_4)_{11}(PO_3OH)F_2$ is a new member of the

*E-mail: msminerals@gmail.com
https://doi.org/10.1180/minmag.2017.081.066

arrojadite group. It was found at the dump of Elisabeth adit near Gemerská Poloma village, Rožňava Co., Košice Region, Slovak Republic.

The new mineral is named according to the nomenclature scheme of arrojadite-group minerals (Chopin *et al.*, 2006), which was approved by the International Mineralogical Association Commission on New Minerals, Nomenclature and Classification (IMA-CNMNC) and it is based on the occupancy of *M* (root-name), *A*1 (first suffix), *B*1 (second suffix) and *W* (first prefix) sites. Three root-names are recognized for arrojadite-group minerals: arrojadite (Fe^{2+} dominant at *M* sites), dickinsonite (Mn^{2+} dominant at *M* sites) and carmoite (Mg dominant at the *M* sites; Cámara *et al.*, 2015). The general structural formula for arrojadite-group minerals is $A_2B_2CaNa_{2+x}M_{13}Al(PO_4)_{11}(PO_3OH_{1-x})W_2$ (for details see Chopin *et al.*, 2006). In fluorarrojadite-(BaNa) Fe^{2+} is the dominant cation at the *M* site (so the root-name is arrojadite) and two suffixes are added to the root-name according to the dominant cation of the dominant valence state at the *A*1 (Ba^{2+}) and *B*1 sites (Na^{+}). The prefix fluor is added to the root-name as F^{-} is dominant over $(OH)^{-}$ at the *W* site.

The new mineral and the name were approved by the CNMNC (IMA 2016-075; Števko *et al*., 2016). The description of fluorarrojadite-(BaNa) is based upon two holotype specimens (two parts of one large piece). One is deposited in the collections of the Department of Mineralogy and Petrology, National Museum in Prague, Cirkusová 1740, 19300 Praha 9, Czech Republic under the catalogue number P1P 13/2016. The second holotype specimen is deposited in the collections of the Department of Mineralogy and Petrology, Faculty of Natural Sciences, Comenius University, Ilkovičova 6, 84215 Bratislava IV, Slovak Republic under the catalogue number 7401.

Occurrence

Several specimens with fluorarrojadite-(BaNa) were found at the dumps of Elisabeth adit (which exploited the Gemerská Poloma talc deposit) situated near Gemerská Poloma village, Rožňava Co., Košice Region, Slovak Republic (48° 45'04.06''N, 20°29'39.27''E). During the exploration of the talc-magnesite deposit the main crosscut of the Elisabeth adit intersected a large body of specialized S-type granite (also called Gemeric granite) with abundant hydrothermal quartz veins containing fluorarrojadite-(BaNa).

The granitic rocks of the Gemeric Unit represent a distinct type of specialized (Sn–W–F), highly evolved suite with S-type affinity, which differs from other granitoids occurring in the Veporic and Tatric Units of the Western Carpathian crystalline basement; they are enriched in phosphorus and rare lithophile elements, such as Li, Rb, Cs, B, Ga, Sn, W, Nb, Ta and U and depleted in rare-earth elements, Zr, Ti, Sr and Ba (e.g. Uher and Broska, 1996; Petrík and Kohút, 1997; Kubiš and Broska, 2005, 2010; Breiter *et al.*, 2015). The Gemeric granitic rocks form several small plutons intruded into the intensively folded Lower Paleozoic (mainly Ordovician to Devonian) volcano-sedimentary complex of the Gelnica Group, metamorphosed in the greenschist metamorphic facies (Bajaník *et al.*, 1984; Petrasová *et al.*, 2007). In the Gemerská Poloma area, the metamorphic rocks are composed mainly of phyllites, metapyroclastic rocks of rhyolitic to dacitic composition, locally with lenses of metadolomite, and strongly steatitized magnesite with a recently exploited talc deposit near Gemerská Poloma (Kilík, 1997). The age of the granite intrusion and related hydrothermal veins with fluorarrojadite-(BaNa) and other phosphates is Late Permian (~260 to 250 Ma), on the basis of zircon U–Pb radiometric age determination of the granites (Poller *et al.*, 2002) and Re–Os molybdenite dating of related Sn–W–Mo mineralization (Kohút and Stein, 2005).

Several types of the Gemeric granites were distinguished at the Gemerská Poloma area: (1) coarse-grained porphyritic granite to granite porphyry; (2) medium-grained Li-annite-topaz-tourmaline bearing granite; (3) P-enriched topaz-zinnwaldite leucogranite; and (4) albitite (Dianiška *et al*., 2002, 2007; Petrík *et al.*, 2014; Breiter *et al.*, 2015). Except for albitites, all the other granite types were encountered recently in the Elisabeth adit (Števko *et al*., 2015).

The hydrothermal quartz veins with albite, muscovite, fluorite, siderite, calcite, dolomite, sulfides and sulfosalts were observed in all types of granite, but the occurrence of the quartz veins with fluorarrojadite-(BaNa) and other phosphates (fluorapatite, 'fluordickinsonite-(BaNa)', triplite and viitaniemiite) is limited only to the highly fractionated topaz–zinnwaldite leucogranite (Števko *et al.*, 2015). The quartz veins with fluorarrojadite-(BaNa) are up to 8 cm thick and no more than 3 m long and except for other phosphates (common and macroscopic: fluorapatite and triplite; rare and microscopic: viitaniemiite; very rare and microscopic: 'fluordickinsonite-(BaNa)') they contain minor

amounts of albite, orthoclase, muscovite, fluorite, Mn-rich siderite to rhodochrosite, arsenopyrite, pyrite, bismuthinite, kobellite, tintinaite, giessenite and native bismuth.

Physical and optical properties

Fluorarrojadite-(BaNa) occurs as very fine grained irregular aggregates usually up to 1 cm x 1 cm in size, exceptionally up to 4 cm x 2 cm (Fig. 1), which consists of individual anhedral grains up to 0.01 mm. Individual crystals have not been observed. It has a yellowish-brown to greenish-yellow colour, very pale yellow streak, a vitreous to greasy lustre and is non-fluorescent in SW and LW ultraviolet light. The Mohs hardness is estimated at ~4½ to 5 based upon scratch tests and by analogy to other arrojadite-group minerals. The fracture is irregular and tenacity is brittle. No cleavage was observed as aggregates of fluorarrojadite-(BaNa) are fine grained. The measured density acquired by floating of the mineral fragments in a mixture of the Clerici solution (density 4.2 g cm^{-3}) and distilled water is 3.61(2) g cm^{-3}, whereas calculated density is 3.650 g cm^{-3} based on the empirical formula and unit-cell volume. Fluorarrojadite-(BaNa) is optically biaxial (+) without apparent pleochroism. Refractive indexes and other optical properties were not determined due to the very small grain size of single crystals. The calculated refractive index based on the empirical formula is 1.674.

Raman spectroscopy

The Raman spectrum of fluorarrojadite-(BaNa) was collected in the range 3580–50 cm^{-1} using a DXR dispersive Raman Spectrometer (Thermo Scientific) mounted on confocal Olympus microscope at the Department of Mineralogy and Petrology, National Museum, Prague, Czech Republic. The Raman signal was excited by a green 532 nm diode-pumped solid-state laser and detected by a CCD detector. The experimental parameters were: 10x objective, 1 s exposure time, 1000 exposures, 900 lines/mm grating, 50 μm slit spectrograph aperture and 8 mW laser power level. The instrument was set up by a software-controlled calibration procedure using multiple neon emission lines (wavelength calibration), multiple polystyrene Raman bands (laser frequency calibration) and standardized white-light sources (intensity calibration). Spectral manipulations were performed using the *Omnic 9* software (Thermo Scientific).

The Raman spectrum (Fig. 2) of fluorarrojadite-(BaNa) is similar to spectra published by Frost *et al.* (2013) for arrojadite-(KFe) and those on the RRUFF database (www.rruff.info, Lafuente *et al.*, 2015): arrojadite-(KNa) (R050107), arrojadite-(KFe) (R070319) and arrojadite-(NaFe) (R070298). The existence of several non-equivalent $(PO_4)^{3-}$ groups, their strong distortion and the presence of the $(PO_3OH)^{2-}$ group in the crystal structure of the proposed new mineral leads to a complex Raman spectrum with a lot of overlapping bands corresponding to stretching and bending vibrations of phosphate groups (Nakamoto, 1986). The most intensive bands in the region 1060–830 cm^{-1} (1020, 985, 959, 939, 916 and 839 cm^{-1}) corresponds to the ν_1 symmetric stretching vibration of $(PO_4)^{3-}$ and $(PO_3OH)^{2-}$ groups; those at 1151, 1113 and 1076 cm^{-1} to ν_3 antisymmetric stretching vibration of $(PO_4)^{3-}$ and $(PO_3OH)^{2-}$ groups. The bending vibrations of $(PO_4)^{3-}$ and $(PO_3OH)^{2-}$ groups

FIG. 1. Yellowish-brown fine grained aggregate of fluoarrojadite-(BaNa) associated with minor dark green grains of fluorapatite in quartz matrix. Field of view is 40 mm. Photo: Pavel Škácha.

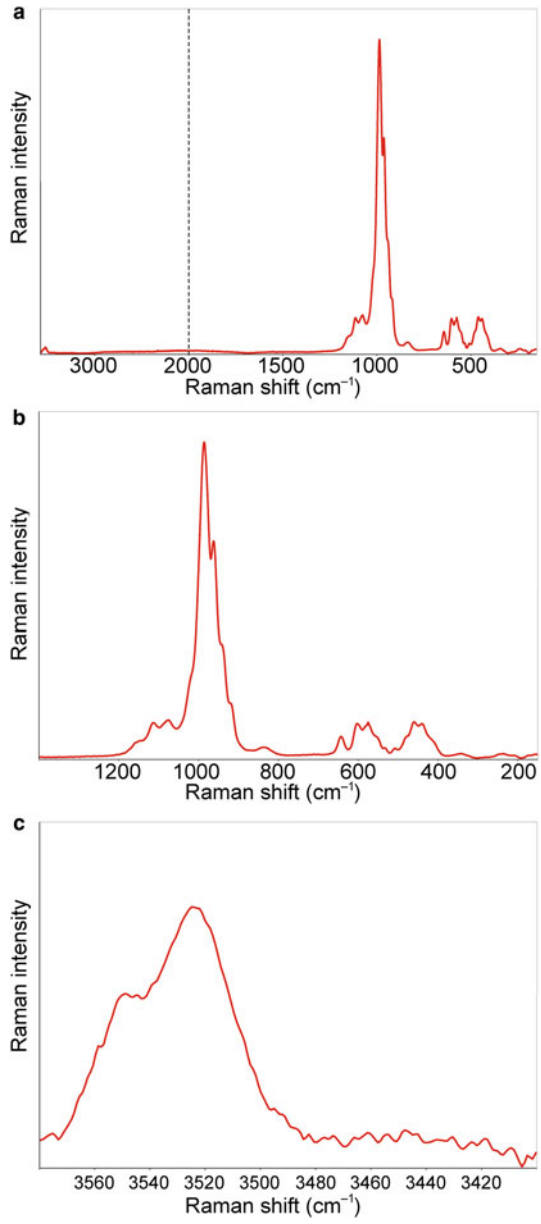

FIG. 2. (*a*) Raman spectrum of fluorarrojadite-(BaNa) from Gemerská Poloma, full range. (*b*) 150–1400 cm^{-1}. (*c*) 3400–3580 cm^{-1}.

are represented by bands in the region with frequencies between 700 and 400 cm^{-1}: 507, 481, 461, 439 and 414 cm^{-1} (ν_2) and 643, 602, 580, 575, 551 and 532 cm^{-1} (ν_4). The observed bands at 3551 and 3523 cm^{-1} are connected to stretching vibrations of OH groups. These compare well with stretching vibrations observed by Cámara *et al.* (2006) in Nickel Plate mine arrojadite-(KFe) and Rapid Creek arrojadite-(KNa) and also with Fourier-transform infrared spectroscopy absorbance data by Della

Ventura *et al.* (2014) for Nickel Plate mine arrojadite-(KFe). Note, the absence of molecular water in the mineral phase studied is confirmed by a lack of observed bands in the region 1650–1550 cm^{-1}.

Chemical composition

Quantitative chemical analyses (5 points) of fluorarrojadite-(BaNa) were performed at the Laboratory of Electron Microscopy and Microanalysis of the Masaryk University and Czech Geological Survey in Brno, Czech Republic on a Cameca SX100 electron microprobe equipped with five wavelength-dispersive spectrometers (WDS). Analytical conditions were: 15 kV accelerating voltage, 10 nA beam current, 10 µm beam diameter and WDS mode. Raw X-ray intensities were corrected for matrix effects with a φ(ρz) algorithm (Pouchou and Pichoir, 1991).

The contents of trace elements in fluorarrojadite-(BaNa) were determined by laser ablation inductively coupled plasma mass spectrometry (LA-ICP-MS) at the Department of Chemistry, Faculty of Science, Masaryk University, Brno, Czech Republic. The setup consists of laser ablation system UP213 (New Wave, USA) and quadrupole ICP-MS Agilent 7500ce (Agilent Technologies, Japan). The ablation system is equipped with Nd:YAG laser emitting radiation with a wavelength of 213 nm. Laser ablation was performed with a single hole drilling mode for the duration of 60 s for each spot of 100 µm diameter with a laser fluency of 12 J cm^{-2} and repetition rate of 10 Hz. The LA-ICP-MS measurements were normalized on average electron-microprobe measured concentration of phosphorus in fluorarrojadite-(BaNa) and the NIST SRM 610 glass reference material was used. Analytical data for fluorarrojadite-(BaNa) as well as standards used are given in Table 1 and the LA-ICP-MS analyses of selected trace elements in fluorarrojadite-(BaNa) are given in Table 2.

On the basis of 47 O OH + F = 2 + [21 – the sum of non-(P,Al) cations] atoms per formula unit (apfu) (Chopin *et al.*, 2006) the average composition of fluorarrojadite-(BaNa) corresponds to the empirical formula: $(Na_{3.96}Ca_{0.74}Ba_{0.69}K_{0.35}Sr_{0.20}Pb_{0.02})_{\Sigma 5.96}{}^{M}(Fe_{7.62}Mn_{5.17}Li_{0.37}Mg_{0.12}Sc_{0.08}Zn_{0.06}Ti_{0.02}Ga_{0.02})_{\Sigma 13.46}Al_{1.02}(P_{12.02}O_{47})(F_{1.54}OH_{1.00}O_{0.46})_{\Sigma 3.00}$. The elements have been grouped into four categories: large low-charge cations (alkali and

TABLE 1. Chemical composition (in wt.%) of fluorarrojadite-(BaNa).

Constituent	Mean	Range	SD	Standard
K_2O	0.76	0.70–0.86	0.07	sanidine
Na_2O	5.72	5.52–5.84	0.36	albite
Li_2O*	0.26	0.26		NIST SRM 610
BaO	4.91	4.02–5.73	0.18	baryte
SrO	0.98	0.70–1.36	0.18	$SrSO_4$
CaO	1.93	1.85–2.01	0.08	fluorapatite
PbO	0.23	0.12–0.38	0.12	vanadinite
MgO	0.23	0.21–0.24	0.03	Mg_2SiO_4
ZnO	0.22	0.19–0.24	0.11	gahnite
MnO	17.08	16.86–17.32	0.46	spessartine
FeO	25.51	25.21–26.15	0.55	almandine
Al_2O_3	2.43	2.31–2.50	0.09	sanidine
Sc_2O_3*	0.26	0.26		NIST SRM 610
Ga_2O_3*	0.08	0.08		NIST SRM 610
TiO_2	0.07	0.05–0.10	0.02	titanite
P_2O_5	39.75	39.21–40.26	0.50	fluorapatite
F	1.36	1.30–1.46	0.11	topaz
H_2O**	0.47			
O = F	−0.57			
Total	101.67			

* Obtained by LA-ICP-MS; ** calculated as (F + OH + Na3) = 3 apfu; SD = standard deviation.

TABLE 2. Trace element LA-ICP-MS analyses of fluorarrojadite-(BaNa) from Gemerská Poloma (in ppm).

#	1	2	3	4	5	6	7	8	9	10	11	12	13	14	15	Average	d.l.
Li	1178	1204	1203	1347	1200	1076	1106	1424	1293	1283	1155	1081	1206	1143	942	1189	0.2
Be	2.2	2.9	2.2	3.5	2.5	1.9	2.6	2.3	2.2	2.1	3.9	3.0	2.6	3.1	2.3	2.6	0.1
B	10	9.0	8.5	10	9.3	6.7	8.2	12	6.5	6.0	5.7	5.3	6.5	6.5	4.8	7.7	1.6
Sc	1458	1384	1483	1150	1146	1885	1656	2183	1754	1741	1258	1472	1944	2081	1755	1623	0.2
Ti	299	367	337	328	310	285	273	360	339	302	292	282	336	315	284	314	0.4
V	<	<	<	<	<	<	<	<	<	<	<	<	<	<	<	<	0.1
Cr	1.4	<	1.3	1.9	0.6	<	<	1.0	<	<	2.4	0.6	<	<	<	1.3	0.3
Co	0.5	0.4	0.4	3.1	0.5	0.2	0.4	0.6	0.7	0.5	0.4	0.3	0.4	0.3	0.4	0.6	0.1
Cu	2.3	1.6	1.7	2.6	2.0	2.2	1.8	3.6	2.1	2.2	1.6	2.0	3.3	2.7	2.5	2.3	0.3
Ga	541	545	693	560	562	642	609	709	621	636	511	524	555	673	621	600	0.1
Ge	64	67	73	62	63	54	53	59	49	46	47	41	41	44	39	53	0.1
Rb	47	57	57	73	53	34	39	49	59	45	71	56	50	35	37	51	0.1
Y	14	19	17	19	17	11	14	16	17	14	17	17	14	16	14	16	0.1
Zr	0.7	0.9	0.7	1.0	0.8	0.6	0.8	0.9	0.9	0.6	0.9	0.8	0.8	0.6	0.7	0.8	0.1
Nb	0.7	1.1	0.4	0.6	0.6	0.6	0.6	0.8	0.8	0.5	0.5	0.5	0.6	1.2	0.9	0.7	0.1
Sn	3.0	0.4	<	<	<	<	<	<	<	<	<	0.2	<	2.1	1.1	1.4	0.1
Sb	0.5	0.5	0.5	0.9	0.7	0.5	0.4	0.6	0.5	0.7	0.5	0.5	0.5	0.9	0.5	0.6	0.1
La	1.8	1.1	1.2	1.1	1.0	0.8	0.9	1.0	1.0	1.0	0.7	0.9	0.9	0.8	0.8	1.0	0.1
Ce	4.8	2.8	3.3	3.5	3.2	2.1	2.7	2.8	2.7	2.5	2.5	2.2	2.3	2.3	2.2	2.8	0.1
Pr	<	<	<	<	<	<	<	<	<	<	<	<	<	<	<	<	0.1
Nd	1.3	0.8	1.0	1.3	1.2	0.5	0.8	1.0	0.9	0.6	0.6	0.6	0.7	0.7	0.5	0.8	0.1
Sm	0.5	0.3	0.5	0.4	0.4	0.3	0.3	0.6	0.4	0.4	0.2	0.3	0.3	0.3	0.4	0.4	0.1
Eu	3.5	2.9	3.5	3.2	3.2	2.8	3.5	3.6	2.8	3.3	2.6	2.8	3.1	3.1	3.1	3.1	0.1
Gd	0.6	0.4	0.6	0.7	0.6	0.3	0.5	0.7	0.5	0.4	0.5	0.4	0.5	0.5	0.5	0.5	0.1
Tb	<	<	<	<	<	<	<	<	<	<	<	<	<	<	<	<	0.1
Dy	1.4	1.6	1.8	1.6	1.8	1.3	1.3	1.8	1.8	1.3	1.6	1.6	1.5	1.4	1.4	1.5	0.1
Ho	<	<	<	<	<	<	<	<	<	<	<	<	<	<	<	<	0.1
Er	1.3	1.6	1.7	1.6	1.5	1.0	1.2	1.4	1.3	1.3	1.2	1.3	1.4	1.3	1.2	1.4	0.1
Tm	0.3	0.4	0.5	0.4	0.4	0.3	0.4	0.4	0.4	0.3	0.4	0.4	0.4	0.4	0.3	0.4	0.1
Yb	3.6	4.9	4.6	4.5	4.4	3.0	4.2	4.3	3.7	4.0	3.9	4.0	4.2	4.2	3.6	4.1	0.1
Lu	2.3	1.6	1.7	2.6	2.0	2.2	1.8	3.6	2.1	2.2	1.6	2.0	3.3	2.7	2.5	2.3	0.3
Th	<	<	<	<	<	<	<	<	<	<	<	<	<	<	<	<	0.1
U	1.1	1.4	1.1	1.9	1.3	1.1	1.3	1.8	0.8	0.8	1.5	1.3	0.9	1.8	1.1	1.3	0.1

d.l. = Detection limit; '<' = not detected.

alkaline earth metals plus lead) occupying high coordination number sites; small alkali and alkaline earth metals plus transition metals in four-, five- and six-fold coordinated sites; Al (Ga) in small octahedra and P in tetrahedral coordination. The sum of [Fe + Mn + Mg + Li+(Sc,Zn,Ti)] > 13 apfu, but it is < 13.5 therefore precluding dominance of Fe (or Mn) in the *B*1b,c sites described by Chopin *et al.* (2006). In addition, the sum of alkali and alkali earths metals is close to 6 apfu. Of them 1.69 are divalent cations (essentially Ca and Ba), and this implies that the formula scheme has to be no. 3 in table 3 of Chopin *et al.* (2006). Therefore, Ba must be dominant at the *A*1 site and Na at the *B*1 site. Furthermore, the analysed fluorine content is F > 1.5 apfu, distinguishing it from the composition reported by Vignola *et al.* (2015), and thus this mineral has to be classified as fluorarrojadite-(BaNa).

In the absence of site partitioning that can be obtained only from crystal-structure refinement (see below), site assignment follows the cation ordering scheme proposed by Cámara *et al.* (2006), allowing the ordering of the cations to be guessed in the different sites of the structure, thus leading to the following crystal-chemical formula: $^{A1}(Ba_{0.65}K_{0.35})_{\Sigma1.00}$ $^{A2}Na_{0.35}$ $^{B1}(Na_{0.54}Fe_{0.46})_{\Sigma1.00}$ $^{B2}Na_{0.54}$ $^{Ca}(Ca_{0.74}Sr_{0.20}Pb_{0.02}Ba_{0.04})_{\Sigma1.00}$ Na_2 $^{Na3}Na_{0.46}$ $^{M}(Fe_{7.16}Mn_{5.17}Li_{0.37}Mg_{0.12}Sc_{0.08}Zn_{0.06}Ga_{0.02}Ti_{0.02})_{\Sigma13.00}Al_{1.02}P_{11}O_{44}$ $PO_{3.46}(OH)_{0.54}$ $^{W}(F_{1.54}OH_{0.46})_{\Sigma2.00}$. The presence of 0.46 apfu of Fe^{2+} at *B*1 sites implies that *B*2 can be at most occupied by 0.56 apfu of Na, the remaining Na partially occupying the Na3 site. This implies that in the calculation of total amount of (F + OH), the Na present at the Na3 site must be subtracted to 3 (F + OH), because the occupancy of the Na3 site is incompatible with a proton bonded to the O3x anion site at the PO_4 group at the P1x site (see Cámara *et al.*, 2006 for a discussion of local ordering). Although the Raman spectrum does not show a clear indication of a deprotonation of the PO_4 group, there is other evidence from crystal data that supports this site assignment (see below). The ideal, fully ordered end-member formula of fluorarrojadite-(BaNa) is $^{A1}Ba^{A2}\square^{B1}Na^{B2}Na^{Ca}Ca^{Na1}Na^{Na2}Na^{Na3}\square^{M}Fe_{13}Al(PO_4)_{11}(PO_3OH)^{W}(F)_2$, which can be simplified as $BaNa_4CaFe_{13}Al(PO_4)_{11}(PO_3OH)F_2$, and requires Na_2O 5.63, BaO 6.97, CaO 2.55, FeO 42.44, Al_2O_3 2.32, P_2O_5 38.69 F 1.73, H_2O 0.41 and O = F –0.73, total 100.00 wt.%. The holotype material studied was homogenous, but some of earlier collected samples from Gemerská Poloma studied by Števko *et al.* (2015) suggest that a complete solid-solution exists between fluorarrojadite-(BaNa) and arrojadite-(BaNa), following a simple $F^- \leftrightarrow (OH)^-$ substitution. Likewise, a solid solution exists between fluorarrojadite-(BaNa) and an as yet unapproved new member of the arrojadite group 'fluordickinsonite-(BaNa)'.

X-ray diffraction data

Single-crystal X-ray studies of fluorarrojadite-(BaNa) were not carried out because of the absence of suitable single crystals: as the material studied is very fine grained (individual grains up to 0.01 mm) and several attempts to obtain a suitable single crystal from the fine-grained mass of fluorarrojadite-(BaNa) were unsuccessful.

Powder X-ray diffraction data for fluorarrojadite-(BaNa) were recorded using a Bruker D8 Advance diffractometer equipped with solid-state LynxEye detector and secondary monochromator producing Cu*K*α radiation housed at the Department of Mineralogy and Petrology, National Museum, Prague, Czech Republic. The instrument was operating at 40 kV and 40 mA. In order to minimize the background, the powdered sample was placed on the surface of a flat silicon wafer in ethanol suspension. The powder pattern was collected in the Bragg–Brentano geometry in the range 3–75° 2θ, with 0.01° step size and a counting time of 30 s per step (total duration of the experiment was ~3 days). Positions and intensities of diffractions were found and refined using the Pearson VII profile-shape function of the *ZDS* program package (Ondruš, 1993) and the unit-cell parameters were refined by the least-squares program of Burnham (1962). The powder X-ray diffraction data of fluorarrojadite-(BaNa) are given in Table 3. Unit-cell parameters of fluorarrojadite-(BaNa) refined for the monoclinic space group *Cc* are: $a = 16.563(1)$ Å, $b = 10.0476(6)$ Å, $c = 24.669(1)$ Å, $\beta = 105.452(4)°$, $V = 3957.5(4)$ Å^3 and $Z = 4$. The application of Rietveld refinement is highly questionable considering that the structure has >90 independent atom sites. However, we conducted a test using the collected data and the model published by Cámara *et al.* (2006) for arrojadite-(SrFe), allowing for refinement of cation occupancies at *A*1, *A*2, *B*1, Na3 and Ca sites (Ba vs. K and Na; Na vs. Fe and Na; and Na and Ca vs. Sr, respectively). The chemistry at the *M*1 and *M*3 sites was allowed to vary, but was fixed in all the other *M* sites. The atom coordinates of every cation and anion sites in

TABLE 3. X-ray powder diffraction data of fluorarrojadite-(BaNa) from Gemerská Poloma; the strongest diffractions are reported in bold.

$I_{meas.}$	$d_{meas.}$	$d_{calc.}$	h	k	l	$I_{meas.}$	$d_{meas.}$	$d_{calc.}$	h	k	l	$I_{meas.}$	$d_{meas.}$	$d_{calc.}$	h	k	l
1	8.506	8.504	1	1	0	12	2.5959	2.5965	1	3	$\overline{6}$	9	1.7577	1.7579	6	4	2
2	7.638	7.634	2	0	$\overline{2}$	**33**	**2.5563**	**2.5583**	**0**	**2**	**8**	4	1.7551	1.7563	8	0	4
3	7.436	7.433	1	1	$\overline{2}$	**33**	**2.5563**	**2.5558**	**4**	**2**	**4**	4	1.7551	1.7551	7	1	6
1	6.494	6.495	1	1	2	8	2.5447	2.5446	6	0	$\overline{6}$	3	1.7287	1.7288	6	2	$\overline{12}$
5	5.940	5.945	0	0	4	**23**	**2.5117**	**2.5119**	**0**	**4**	**0**	1	1.7149	1.7146	3	5	$\overline{7}$
4	5.527	5.524	2	0	$\overline{4}$	5	2.4204	2.4202	4	2	$\overline{8}$	1	1.7135	1.7138	5	5	$\overline{1}$
5	5.235	5.233	1	1	$\overline{4}$	9	2.4181	2.4175	6	2	$\overline{2}$	1	1.7135	1.7130	1	1	$\overline{14}$
6	5.023	5.024	0	2	0	7	2.3875	2.3870	6	2	$\overline{4}$	2	1.7104	1.7099	4	4	$\overline{10}$
7	4.775	4.774	3	1	$\overline{2}$	2	2.3570	2.3570	3	1	$\overline{10}$	4	1.7008	1.7008	5	5	0
5	4.704	4.703	3	1	0	3	2.3377	2.3375	6	2	$\overline{5}$	3	1.6819	1.6819	1	5	$\overline{8}$
11	4.627	4.628	0	2	2	1	2.3118	2.3111	5	3	0	2	1.6788	1.6787	5	1	10
14	4.577	4.578	1	1	4	1	2.2970	2.2970	1	3	7	2	1.6749	1.6750	5	3	8
2	4.253	4.252	2	2	0	1	2.2641	2.2635	4	2	$\overline{9}$	8	1.6606	1.6609	3	5	$\overline{8}$
5	4.198	4.200	3	1	$\overline{4}$	3	2.2568	2.2565	5	3	$\overline{5}$	8	1.6606	1.6605	2	2	$\overline{14}$
1	4.196	4.197	2	2	$\overline{2}$	8	2.1985	2.1983	7	1	$\overline{6}$	3	1.6582	1.6582	0	6	2
1	4.128	4.130	4	0	$\overline{2}$	5	2.1494	2.1494	0	2	10	3	1.6582	1.6579	8	2	4
2	4.058	4.059	3	1	2	4	2.1458	2.1461	4	4	$\overline{2}$	5	1.6567	1.6563	1	3	12
1	3.962	3.963	0	0	6	5	2.1268	2.1260	4	4	0	2	1.6308	1.6310	1	5	8
6	3.837	3.837	0	2	4	3	2.1218	2.1217	0	4	6	4	1.6223	1.6222	3	1	$\overline{15}$
6	3.837	3.835	2	2	2	3	2.0910	2.0906	7	1	2	4	1.6223	1.6222	1	1	14
1	3.542	3.544	2	2	3	2	2.0554	2.0549	7	1	$\overline{8}$	8	1.6124	1.6124	4	0	12
1	3.512	3.513	4	0	2	3	2.0295	2.0296	6	2	4	2	1.5939	1.5944	10	0	$\overline{8}$
5	3.457	3.458	3	1	$\overline{6}$	7	1.9942	1.9958	8	0	0	2	1.5939	1.5936	7	1	8
5	3.457	3.454	0	2	5	8	1.9770	1.9771	1	5	$\overline{2}$	5	1.5770	1.5770	6	0	10
21	**3.412**	**3.412**	**1**	**1**	**6**	11	1.9601	1.9606	2	2	10	2	1.5615	1.5626	8	4	0
12	3.328	3.328	3	1	4	11	1.9601	1.9597	4	2	8	3	1.5596	1.5602	8	2	$\overline{12}$
2	3.277	3.278	1	3	0	3	1.9429	1.9428	2	4	$\overline{8}$	3	1.5596	1.5589	10	2	$\overline{6}$
2	3.271	3.271	1	3	$\overline{1}$	1	1.9288	1.9287	7	3	$\overline{2}$	6	1.5336	1.5335	4	6	$\overline{4}$
6	3.247	3.248	2	2	4	2	1.9255	1.9258	7	1	4	2	1.5268	1.5269	7	5	$\overline{4}$
37	**3.224**	**3.225**	**2**	**0**	**6**	3	1.9204	1.9201	3	3	8	2	1.5268	1.5268	10	0	$\overline{10}$
8	3.205	3.205	1	3	$\overline{2}$	3	1.9190	1.9186	0	4	8	1	1.5197	1.5197	10	2	$\overline{8}$
10	3.126	3.129	2	2	$\overline{6}$	4	1.9180	1.9176	4	4	4	1	1.5197	1.5196	8	4	$\overline{8}$
10	3.126	3.124	3	1	$\overline{7}$	8	1.9086	1.9085	8	0	$\overline{8}$	4	1.4863	1.4866	5	5	$\overline{10}$
100	**3.040**	**3.039**	**4**	**2**	$\overline{4}$	3	1.8852	1.8852	7	3	0	4	1.4863	1.4862	2	6	6
5	2.9720	2.9726	0	0	8	7	1.8580	1.8583	4	4	$\overline{8}$	3	1.4698	1.4703	9	1	$\overline{13}$
3	2.9386	2.9391	1	3	$\overline{4}$	7	1.8580	1.8571	6	4	$\overline{2}$	3	1.4698	1.4691	11	1	$\overline{7}$

1	2.9226	2.9216	5	1	$\bar{5}$	1	1.8436	1.8443	5	3	$\bar{10}$	3	1.4698	1.4694	2	2	$\bar{16}$
4	2.8791	2.8788	4	2	2	1	1.8436	1.8431	6	4	$\bar{4}$	3	1.4638	1.4633	10	2	2
22	**2.8499**	**2.8499**	**3**	**3**	$\bar{\mathbf{2}}$	2	1.8428	1.8429	1	1	$\bar{13}$	2	1.4589	1.4590	0	6	8
18	2.8327	2.8346	3	3	0	2	1.8428	1.8412	6	0	$\bar{12}$	2	1.4589	1.4585	4	6	4
1	2.8308	2.8312	3	1	$\bar{8}$	1	1.8265	1.8277	7	3	$\bar{7}$	2	1.4411	1.4411	2	4	$\bar{14}$
11	2.8062	2.8064	1	3	4	1	1.8265	1.8266	6	4	0	2	1.4318	1.4318	4	0	14
9	2.7782	2.7778	5	1	$\bar{6}$	3	1.8019	1.8017	7	3	2	2	1.4294	1.4295	1	5	$\bar{12}$
17	2.7619	2.7618	4	0	$\bar{8}$	2	1.7799	1.7799	9	1	$\bar{6}$	2	1.4294	1.4295	4	4	$\bar{14}$
11	2.7580	2.7579	6	0	$\bar{2}$	2	1.7799	1.7795	8	0	$\bar{10}$	5	1.4253	1.4250	6	6	$\bar{4}$
56	**2.7135**	**2.7138**	**2**	**2**	**6**	1	1.7721	1.7718	4	4	6	5	1.4253	1.4252	0	2	16
5	2.6732	2.6733	3	3	2	14	1.7596	1.7596	2	4	$\bar{10}$	4	1.4236	1.4235	8	2	8
3	2.6166	2.6165	2	2	$\bar{8}$	14	1.7596	1.7594	2	0	$\bar{14}$	1	1.4145	1.4156	6	2	$\bar{16}$

The eight strongest lines are given in bold.

the structure were kept fixed. Refinement was performed with *GSAS* + *EXPGUI* software (Larson and Von Dreele, 1994; Toby, 2001). The residuals improved sensibly ($wR_p = 0.0398$, wR_p after background subtraction 0.0911; $R(F^2) = 0.1475$) when chemistry was allowed to vary in the above reported sites. Obviously, the results should interpreted with caution. Nevertheless the trend agrees well with what was expected from the formula obtained on the basis of crystal-chemical criteria. Occupancy at *M*1 was determined to be 18.0(7) electrons per site (eps), as expected for fractionation of Li at this site already found in dickinsonite-(KMnNa) by Cámara *et al.* (2006). Zn seems to order in the *M*3 site that is among the smaller octahedra but yielded 29.1(6) eps, evidently overestimated. The most interesting results are obtained for alkali sites: 48.5(4) *vs*. 43.1 eps from chemical formula in the *A*1 site; 2.5(8) *vs*. 3.9 eps from chemical formula in the *A*2 site; 25.7(5) *vs*. 26.3 eps from chemical formula in the Ca site; 22.8(6) *vs*. 17.9 eps from chemical formula in the *B*1 site; and 1.2(7) *vs*. 5.1 eps from chemical formula in the Na3 site. Therefore the worst agreements are found in the *B*1 and Na3 sites, which are usually split sites (see Cámara *et al.*, 2006) thus seriously challenging any plausible satisfactory result. The observed and calculated pattern and the relative residuals are reported in Fig. 3. The results are a reasonable support of the proposed crystal-chemical formula.

Relationship to the known species and origin

As mentioned previously, fluorarrojadite-(BaNa) is a member of the arrojadite group (Cámara *et al.*, 2006; Chopin *et al.*, 2006). Its existence was noted in samples of fluoarrojadite-(BaFe) from the Sidi-bou-Kricha pegmatite in Morocco by Chopin *et al.* (2006) and it was also described as a product of the hydrothermal alteration of triphylite from the Nanping No. 31 granitic pegmatite in Fujian Province, China by Rao *et al.* (2014). The sample studied has a rather high content of Mn^{2+}, among the highest reported for arrojadites in the literature. Only the sample from Buranga (Rwanda) (von Knorring, 1969) has a higher Mn-content and as such it is very close to be classified as a dickinsonite. It is not surprising that in the same locality (Gemerská Poloma) some minute crystals showed compositions classifiable as 'fluordickinsonite-(BaNa)' (Števko *et al.*, 2015). The Mg content is fairly low (only 0.12 apfu),

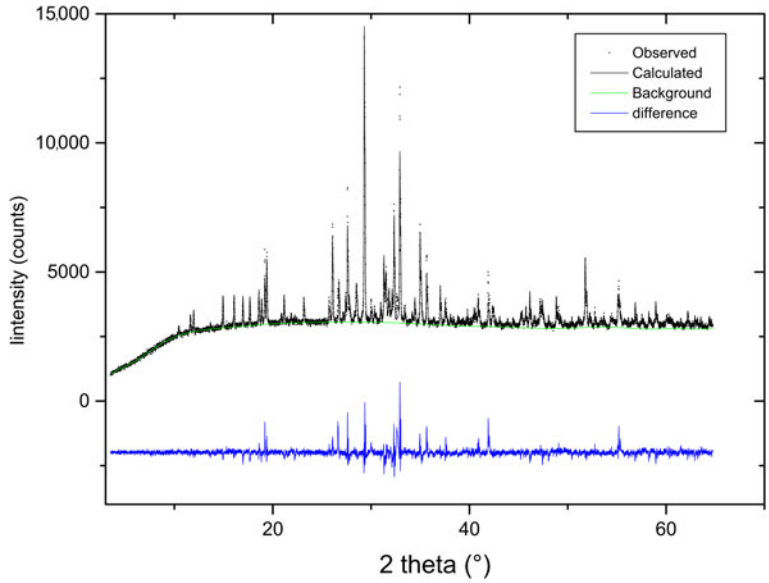

FIG. 3. Observed powder pattern of fluorarrojadite-(BaNa). The calculated intensities, substracted background and residuals obtained by Rietveld refinement (see text) are also reported.

lower than in most of the analyses reported for arrojadites, and far from arrojadite-(PbFe) from Sapucaia (Moore and Ito, 1979) which contains 3.49 apfu of Mg and arrojadite-(BaFe) from Spluga (Demartin *et al.*, 1996) which reaches 5.54 apfu of Mg, but still far from being classifiable as carmoite-(BaFe). Another interesting chemical feature is the presence of significant Li (0.37 apfu), not uncommon in arrojadite-group minerals, although far lower than the amount present in arrojadite-(PbFe) from Sapucaia (0.86 apfu, data from Cámara *et al.*, 2006).

In the Strunz mineral classification system fluorarrojadite-(BaNa) fits in subdivision 8.BF: phosphates, arsenates, vanadates with additional anions, without H_2O, with medium-sized and large cations and (OH, etc.): $RO_4 < 0.5:1$ (Strunz and Nickel, 2001). The comparison of physical properties of the valid mineral species of the arrojadite subgroup are given in Table 4. The observed lattice parameters are among the largest of the arrojadite subgroup and this is due to the fairly low Mg content. In general, all the cell dimensions are correlated negatively with the Mg content. The value observed for the β angle deviates from the positive trend observed by Cámara *et al.* (2006), which compares the value of the β angle with the (Na + K) content (see their Fig. 1), for samples with a vacant Na3 site. This indication is in support of the presence of Na at the Na3 site as suggested by the site assignment on the basis of crystal-chemical criteria and the weak evidence from Rietveld refinement of the presence of some occupation at this site.

Fluorarrojadite-(BaNa) and associated phosphates in quartz veins were formed from late-magmatic to early-hydrothermal P- and F-rich fluids, related to the adjacent granite. These relatively high-temperature fluids altered primary magmatic minerals of the granite (especially albite, K-feldspar, Li-rich micas and fluorapatite) and liberated elements (such as Na, K, Fe, Mn, Ca, Ba, Sr and P) necessary for precipitation of the phosphate minerals.

Acknowledgements

The helpful comments of Jakub Plášil, Peter Leverett and Christian Chopin are greatly appreciated. Pavel Škácha is acknowledged for photography. FC thanks Marco Merlini (Università di Milano, Italy) for help with *GSAS-EXPGUI*. This study was supported financially by the Ministry of Culture of the Czech Republic (DKRVO 2017/02; National Museum 00023272), by the Slovak Research and Development Agency under the APVV-14-0278 project, and by the Ministry of Education, Slovak Republic, the VEGA-1/0499/16 project.

TABLE 4. Comparison of the physical properties for valid members of the arrojadite group (dickinsonite-group minerals and fluorcarmoite-(BaNa) are not included).

Mineral	fluorarrojadite-(BaNa)	fluorarrojadite-(BaFe)	arrojadite-(BaFe)	arrojadite-(KFe)
Type locality	Gemerská Poloma, Slovakia	Sidi-bou-kricha, Morocco	Spluga Valley, Italy	Nickel Plate Mine, USA
Reference	this work	Chopin *et al.* (2006)	Demartin *et al.* (1996) Chopin *et al.* (2006)	Chopin *et al.* (2006)
Ideal formula	$Ba\square)(Na)_2Ca(Na_2\square)\ Fe_{13}Al(PO_4)_{11}(PO_3OH)\ F_2$	$(Ba\square)(Fe^{2+}\ \square)Ca(Na_2\ \square)\ Fe_{13}Al(PO_4)_{11}(PO_3OH)F_2$	$(Ba\square)(Fe^{2+}\ \square)Ca(Na_2\ \square)\ Fe_{13}Al(PO_4)_{11}(PO_3OH)(OH)_2$	$(KNa)(Fe^{2+}\square)Ca(Na_2\square)\ Fe_{13}Al(PO_4)_{11}(PO_3OH)\ (OH)_2$
Crystal system	monoclinic	monoclinic	monoclinic	monoclinic
Space group	*Cc*	*Cc*	*C*2/*c* or *Cc*	*Cc*
a [Å]	16.563(1)	16.4970(9)	16.406(5)	no data
b [Å]	10.0476(6)	10.0176(5)	9.945(3)	
c [Å]	24.669(1)	24.6359(13)	24.470(5)	
β [°]	105.452(4)	105.649(2)	105.73(2)	
V [Å^3]	3957.5(4)	3920.42(5)	3843(2)	
Z	4	4	4	
Strongest powder X-ray diffractions				
	3.412/21	3.4003/31.2	3.010/100*	no data
	3.224/37	3.2108/47.5	3.178/51	
	3.040/100	3.0319/100	2.678/42	
	2.8499/22	2.8413/34.1	2.523/27	
	2.7135/56	2.8285/30.0	2.805/25	
	2.5563/33	2.7595/32.9	2.775/21	
	2.5117/23	2.7031/68.5	2.741/21	
		2.5433/38.1	2.732/21	
Density	3.650 g.cm^{-3}	3.650 g.cm^{-3}	3.544 g.cm^{-3}	no data
Colour	yellowish-brown to greenish-yellow	dark yellowish-green	greyish green	dark yellowish-green

TABLE 4. (*contd.*)

Mineral	arrojadite-(KNa)	arrojadite-(PbFe)	arrojadite-(SrFe)	arrojadite-(BaNa)
Type locality	Rapid Creek, Canada	Sapucaia, Brazil	Horrsjöberg, Sweden	Luna, Dorio, Italy
Reference	Cámara *et al.* (2006)	Chopin *et al.* (2006)	Cámara *et al.* (2006)	Vignola *et al.* (2015)
Ideal formula	(KNa)(Na)Ca(Na_2□) $Fe_{13}Al(PO_4)_{11}(PO_3OH)$ $(OH)_2$	(Pb□)(Fe^{2+}□)Ca(Na_2□) $Fe_{13}Al(PO_4)_{11}(PO_3OH)$ $(OH)_2$	(Sr□)(Fe^{2+}□)Ca(Na_2□) $Fe_{13}Al(PO_4)_{11}(PO_3OH)$ $(OH)_2$	$BaNa_3$(NaCa) $Fe_{13}Al(PO_4)_{11}(PO_3OH)(OH)_2$
Crystal system	monoclinic	monoclinic	monoclinic	monoclinic
Space group	*Cc*	*Cc*	*Cc*	*C*2/*c*
a [Å]	16.5220(11)	16.4304(9)	16.3992(7)	16.4984(6)
b [Å]	10.0529(7)	9.9745(5)	9.9400(4)	10.0228(3)
c [Å]	24.6477(16)	24.5869(13)	24.4434(11)	24.648(1)
β [°]	106.509(2)	105.485(2)	105.489(1)	105.850(4)
V [$Å^3$]	3932.2(7)	3883.2(5)	3839.76(46)	3921
Z	4	4	4	4
Strongest powder X-ray diffractions				
	5.8614/28.8	4.5534/25.1	3.3784/26.2	3.488/28
	5.0264/27.5	3.20882/43.1	3.2931/21.0	3.303/46
	3.1857/33.5	3.0186/100	3.1925/41.2	3.137/100
	3.0498/100	2.8291/35.0	3.0093/100	2.878/32
	2.8529/22.4	2.8196/32.9	2.8202/23.5	2.818/61
	2.7979/24.9	2.7496/29.1	2.8053/28.4	2.667/35
	2.7933/28	2.6982/54.8	2.7370/27.8	
	2.7532/22.8	2.5376/30.4	2.7304/20.1	
	2.6908/71.3		2.6861/69.9	
Density	3.437 $g.cm^{-3}$	3.596 $g.cm^{-3}$	3.569 $g.cm^{-3}$	3.76 $g.cm^{-3}$
Colour	yellow	pale honey	green	pale greyish-green

* data from Demartin *et al.* (1996) for space group *C*2/*c*.

References

Bajaník, Š., Ivanička, J., Mello, J., Pristaš, J., Reichwalder, P., Snopko, L., Vozár, J. and Vozárová, A. (1984) *Geological map of the Slovenské Rudohorie Mts. – Eastern part 1: 50 000*. Dionýz Štúr Institute of Geology, Bratislava.

Breiter, K., Broska, I. and Uher, P. (2015) Intensive low-temperature tectono-hydrothermal overprint of peraluminous rare-metal granite: a case study from the Dlhá dolina valley (Gemericum, Slovakia). *Geologica Carpathica*, **66**, 19–36.

Burnham, C.W. (1962) Lattice constant refinement. *Carnegie Institute Washington Yearbook*, **61**, 132–135.

Cámara, F., Oberti, R., Chopin, C. and Medenbach, O. (2006) The arrojadite enigma: I. A new formula and a new model for the arrojadite structure. *American Mineralogist*, **91**, 1249–1259.

Cámara, F., Bittarello, E., Ciriotti, M.E., Nestola, F., Radica, F. and Bracco, R. (2015) Fluorcarmoite-(BaNa), IMA 2015-062. CNMNC Newsletter No. 27, October 2015, 1229. *Mineralogical Magazine*, **79**, 1229–1236.

Chopin, C., Oberti, R. and Cámara, F. (2006) The arrojadite enigma: II. Compositional space, new members, and nomenclature of the group. *American Mineralogist*, **91**, 1260–1270.

Della Ventura, G., Bellatreccia, F., Radica, F., Chopin, C. and Oberti, R. (2014) The arrojadite enigma III. The incorporation of volatiles: a polarised FTIR spectroscopy study. *European Journal of Mineralogy*, **26**, 679–688.

Demartin, F., Gramaccioli, C.M., Pilati, T. and Sciesa, E. (1996) Sigismundite, $(Ba,K,Pb)Na_3(Ca,Sr)(Fe,Mg,Mn)_{14}Al(OH)_2(PO_4)_{12}$, a new Ba-rich member of the arrojadite group from Spluga Valley, Italy. *Canadian Mineralogist*, **34**, 827–834.

Dianiška, I., Breiter, K., Broska, I., Kubiš, M. and Malachovský, P. (2002) First phosphorous-rich Nb-Ta-Sn-specialised granite from the Carpathians – Dlhá dolina valley granite pluton, Gemeric superunit. *Geologica Carpathica*, **53**, Special Issue (CD-ROM).

Dianiška, I., Uher, P., Hurai, V., Huraiová, M., Frank, W., Konečný, P. and Kráľ, J. (2007) Mineralization of rare-metal granites. Pp. 254–330 in: *Sources of Fluids and Origin of Mineralizations in the Gemeric Unit* (V. Hurai, editor). Open file report, Dionýz Štúr Institute of Geology, Bratislava [in Slovak].

Frost, R.L., Xi, Y., Schol, R. and Campos Horta, L.F. (2013) The phosphate mineral arrojadite-(KFe) and its spectroscopic characterization. *Spectrochimica Acta Part A: Molecular and Biomolecular Spectroscopy*, **109**, 138–145.

Kilík, J. (1997) Geological characteristic of the talc deposit in Gemerská Poloma-Dlhá dolina. *Acta Montanistica Slovaca*, **2**, 71–80 [in Slovak].

Kohút, M. and Stein, H. (2005) Re-Os molybdenite dating of granite-related Sn-W-Mo mineralisation at Hnilec, Gemeric Superunit, Slovakia. *Mineralogy and Petrology*, **85**, 117–129.

Kubiš, M. and Broska, I. (2005) The role of boron and fluorine in evolved granitic rock systems (on the example of the Hnilec area, Western Carpathians). *Geologica Carpathica*, **56**, 193–204.

Kubiš, M. and Broska, I. (2010) The granite system near Betliar village (Gemeric Superunit, Western Carpathians): evolution of a composite silicic reservoir. *Journal of Geosciences*, **55**, 131–148.

Lafuente, B., Downs, R.T., Yang, H. and Stone, N. (2015) The power of databases: the RRUFF project. Pp. 1–30 in: *Highlights in Mineralogical Crystallography* (T. Armbruster and R.M. Danisi, editors). De Gruyter, Berlin.

Larson, A.C. and Von Dreele, R.B. (1994) *General Structure Analysis System (GSAS)*. Los Alamos National Laboratory Report LAUR 86-748.

Moore, P.B. and Ito, J. (1979) Alluaudites, wyllieites, arrojadites: crystal chemistry and nomenclature. *Mineralogical Magazine*, **43**, 227–235.

Nakamoto, K. (1986) *Infrared and Raman Spectra of Inorganic and Coordination Compounds*. J. Wiley and Sons, New York.

Ondruš, P. (1993) A computer program for analysis of X-ray powder diffraction patterns. *Materials Sci. Forum, EPDIC-2,* Enchede, **133–136**, 297–300.

Petrasová, K., Faryad, S.W., Jeřábek, P. and Žáčková, E. (2007) Origin and metamorphic evolution of magnesite-talc and adjacent rocks near Gemerská Poloma, Slovak Republic. *Journal of Geosciences*, **52**, 125–132.

Petrík, I. and Kohút, M. (1997) The evolution of granitoid magmatism during the Hercynian orogen in the Western Carpathians. Pp. 235–252 in: *Geological Evolution of the Western Carpathians* (P. Grecula, D. Hovorka and M. Putiš, editors). Mineralia Slovaca Monograph, Bratislava.

Petrík, I., Čík, Š., Miglierini, M., Vaculovič, T., Dianiška, I. and Ozdín, D. (2014) Alpine oxidation of lithium micas in Permian S-type granites (Gemeric unit, Western Carpathians, Slovakia). *Mineralogical Magazine*, **78**, 507–533.

Poller, U., Uher, P., Broska, I., Plašienka, D. and Janák, M. (2002) First Permian - Early Triassic zircon ages for tin-bearing granites from the Gemeric Unit (Western Carpathians, Slovakia): connection to the post-collisional extension of theVariscan orogen and S-type granite magmatism. *Terra Nova*, **14**, 41–48.

Pouchou, J.L. and Pichoir, F. (1991) Quantitative analysis of homogeneous or stratified microvolumes applying the model "PAP." Pp. 3 l–75 in: *Electron Probe Quantitation* (K.F.J. Heinrich and D.E. Newbury, editors). Plenum Press, New York.

Rao, C., Wang, R.C., Hatert, F. and Baijot, M. (2014) Hydrothermal transformations of triphylite from the Nanping No. 31 pegmatite dyke, southeastern China. *European Journal of Mineralogy*, **26**, 179–188.

Števko, M., Uher, P., Sejkora, J., Malíková, R., Škoda, R. and Vaculovič, T. (2015) Phosphate minerals from the hydrothermal quartz veins in specialized S-type granites, Gemerská Poloma (Western Carpathians, Slovakia). *Journal of Geosciences*, **60**, 237–249.

Števko, M., Sejkora, J., Uher, P. and Cámara, F. (2016) Fluorarrojadite-(BaNa), IMA 2016-075. CNMNC Newsletter No. 34, December 2016, page 1318; *Mineralogical Magazine*, **80**, 1315–1321.

Strunz, H. and Nickel, E.H. (2001) *Strunz Mineralogical Tables. Chemical Structural Mineral Classification System*. 9th edition. E. Scheizerbart'sche Verlagsbuchhandlung (Nägele u. Obermiller), Stuttgart, 870 pp.

Toby, B.H. (2001) EXPGUI, a graphical user interface for GSAS. *Journal of Applied Crystallography*, **34**, 210–213.

Uher, P. and Broska, I. (1996) Post-orogenic Permian granitic rocks in the Western Carpathian–Pannonian area: geochemistry, mineralogy and evolution. *Geologica Carpathica*, **47**, 311–321.

Vignola, P., Hatert, F., Baijot, M., Dal Bo, F., Andò, S., Bersani, D., Risplendente, A. and Vanini, F. (2015) Arrojadite-(BaNa), IMA 2014-071. CNMNC Newsletter No. 23, February 2015, page 55; *Mineralogical Magazine*, **79**, 51–58.

von Knorring, O. (1969) A note on the phosphate mineralisation at the Buranga pegmatite, Rwanda. *Bulletin du Service géologique du Rwanda*, **5**, 42–45.